No-core-melt assessment for Canadian-SCWR under LOCA/LOECC*

WU Pan (吴攀),[1] SHAN Jian-Qiang (单建强),[1] GOU Jun-Li (苟军利),[1,†]
ZHANG Bin (张斌),[1] ZHANG Bo (张博),[1] and WANG He-Nan (王贺南)[1]

[1]*School of Nuclear Science and Technology, Xi'an Jiaotong University, Xi'an, 710049, China*

(Received May 28, 2014; accepted in revised form July 7, 2014; published online April 20, 2015)

The safety analysis code SCTRAN for SCWR (Super Critical Water Reactor) is modified to own the capability to assess the radiation heat transfer with developing a two-dimensional heat conduction solution scheme and incorporating a radiation heat transfer model. The verification of the developed radiation heat transfer model is conducted through code-to-code comparison with CATHENA. The results show that the modified SCTRAN code is successful for that the maximum absolute error and relative error of the surface temperature between results of SCTRAN and CATHENA are 6.1 °C and 0.9%, which are acceptable in temperature prediction. Then, with the modified SCTRAN code, the loss of coolant accident with a total loss of emergency core cooling system (LOCA/LOECC) of Canadian-SCWR is carried out to evaluate its "no-core-melt" concept. The following conclusions are achieved: 1) in the process of LOCA, the decay heat can be totally removed by the radiation heat transfer and the natural convection of the high-temperature coolant, even without an intervention of ECCS (Emergency Core Cooling System); 2) The peak cladding temperature of the fuel pins in the inner and outer rings of the high power group are 1236 °C and 1177 °C respectively, which are much lower than the melting point of the fuel sheath. It indicates that the Canadian-SCWR can achieve "no-core-melt" concept under LOCA/LOECC.

Keywords: Canadian-SCWR, LOCA/LOECC, No-Core-Melt, SCTRAN, Radiation heat transfer

DOI: 10.13538/j.1001-8042/nst.26.020601

I. INTRODUCTION

The Canadian-SCWR is a pressure-tube type supercritical water reactor (SCWR), which is promising to satisfy all the major GIF (Generation IX International Forum) goals on enhanced safety, sustainability, economics, and proliferation resistance [1]. It applies supercritical light water as coolant and subcritical heavy water as moderator. The high efficiency channel (HEC) design is employed to increase the inherent safety of the reactor. This helps the reactor to achieve "no-core-melt" under postulated accident scenarios with a loss of emergency core cooling system, such as LOCA/LOECC (loss of coolant accident, with a coincident loss-of-emergency core cooling), because the radiation heat transfer inside the HEC and the passive heat rejection through the insulator into the low-temperature moderator can remove the decay heat. Safety analysis is required to demonstrate the feasibility for the continuously updated Canadian-SCWR concept. As LOCA/LOECC leads to the total loss of core coolant and the most serious accident results, its safety analysis is an important reference for evaluating the inherent safety of Canadian-SCWR.

Simulations for evaluating and optimizing thermal performance of Canadian-SCWR following LOCA/LOECC was performed by AECL (Atomic Energy of Canada Limited) utilizing CANFLEX bundle [2]. Transient simulation was carried out with an assumed decay power variation. Effects of insulator properties and moderator temperature on the fuel cladding temperature were analyzed. The results show that Canadian-SCWR has the potential to significantly reduce the possibility of core damage frequency. Shan *et al.* [3] performed sub-channel analyses with ATHAS code and radiation heat transfer analyses with CATHENA code of 54-element Canadian-SCWR bundle. The sub-channel analysis results show that the maximum fuel cladding temperatures are 761 °C at BOC (Begin of Cycle) and 808 °C at EOC (End of Cycle). The radiation heat transfer was calculated at different decay power levels and the results indicate that the pressure tube with 54-element fuel bundle can remove about 2% of the rated power to the moderator through radiation heat transfer. Licht and Xu [4] provided simulation results and analyses of 78-element Canadian-SCWR bundle in the process of LOCA/LOECC. The results show that the temperature of fuel sheath with a non-porous insulator remains below the melting temperature for less than 3% of the rated power. There are suggestions proposed by other authors, however, little researches about the "no-core-melt" assessment of Canadian-SCWR have been published.

The previous analyses of Canadian-SCWR mainly focused on the radiation heat transfer, but not the effect of natural convection during LOCA/LOECC. Meanwhile, the transition process from supercritical pressure to subcritical pressure was not simulated in the analyses. In this paper, a two-dimensional heat conduction model and a radiation heat transfer model are incorporated into SCTRAN [5]. The SCTRAN thermal-hydraulic idealization for Canadian-SCWR based on the latest conceptual design utilizing a 64-element fuel bundle is carried out. The LOCA/LOECC is analyzed by considering the effects of radiation and convection in the HEC.

II. MODIFICATION OF SCTRAN

SCTRAN, a safety analysis code developed at Xi'an Jiaotong University, can simulate most accidents for SCWR in-

* Supported by the Doctoral Program of Higher Education of China (No. 20120201110043) and Atomic Energy of Canada Limited(AECL)

† Corresponding author, junligou@mail.xjtu.edu.cn

cluding LOCA [5], thus can be applied to simulate the accidents at both subcritical and supercritical pressures. A homogenous model and a four-equation dynamic slip model are implemented into the code as optional modes for subcritical pressure condition. Its ability to do safety analysis for SCWRs has been verified [5]. It has been applied to analyze the accident consequences of Chinese pressure vessel type concepts, such as CSR1000 [6] and CGNPC SCWR [5]. In order to simulate radiation heat transfer inside the HEC of Canadian-SCWR, a radiation heat transfer model is incorporated into SCTRAN. The fuel pin absorbs different amounts of radiation heat from different directions, which results in prominent circumferential heat conduction in the fuel pin. Therefore, the original one-dimensional heat conduction model in code SCTRAN should be updated to a two-dimensional one.

A. Development of two-dimensional heat conduction model

The differential equation of heat conduction with an internal heat source is given as

$$\rho c_p \frac{\partial T}{\partial t} = \nabla \cdot [\lambda \nabla T] + S, \tag{1}$$

where, ρ is density, c_p is specific heat capacity, T is temperature, t is time, λ is conductivity and S is heat source, The first term at the right side of Eq. (1) is the energy variation with space while the other stands for the heat source in the heat structure.

In the two dimensional polar coordinate, the conduction equation can be rewritten as

$$\rho c_p \frac{\partial T}{\partial t} = \frac{1}{r}\frac{\partial}{\partial r}\left(\lambda \cdot r \frac{\partial T}{\partial r}\right) + \frac{1}{r^2}\frac{\partial}{\partial \varphi}\left(\lambda \frac{\partial T}{\partial \varphi}\right) + S, \tag{2}$$

where, r is the distance in the radial direction, φ is the angle in the circumferential direction . In order to reduce the calculation iteration and guarantee the calculation accuracy simultaneously, a fuel rod is divided into four sectors in the circumferential direction. The mesh layout for the 2D heat conduction is shown in Fig. 1. Points P, N, S, W and E represent the nodes needing temperature calculation. The material properties and temperatures in a half mesh interval are assumed to be constants over a time interval. For the control volume of point P (shadowed in Fig. 1), the internal energy increase equals to the inner heat source plus the heat conducted from the surrounding control volumes. Thus the discrete form of Eq. (2) can be given as

$$\begin{aligned}(\rho c_p)_p \frac{(r_n + r_s)}{2}\frac{\Delta r \Delta\theta}{\Delta t}(T_p - T_p^0) = &\left[\frac{r_n \lambda_n (T_N - T_p)}{(\delta r)_n} - \frac{r_s \lambda_s (T_P - T_S)}{(\delta r)_s}\right]\Delta\theta \\ &+ \left[\frac{\lambda_e (T_E - T_p)}{(\delta\theta)_e r_e} - \frac{\lambda_w (T_P - T_W)}{(\delta\theta)_w r_w}\right]\Delta r + S\Delta V\end{aligned} \tag{3}$$

where, θ is angle in the circumferential direction. The left part of Eq. (3) represents the internal energy increase of the control volume at point P. The first term of the right side is the heat conducted from points N and S. The second term is the heat conducted from points E and W, while the last term denotes the inner heat source. Eq. (3) can be simplified as

$$a_\mathrm{P} T_\mathrm{P} = a_\mathrm{E} T_\mathrm{E} + a_\mathrm{W} T_\mathrm{W} + a_\mathrm{N} T_\mathrm{N} + a_\mathrm{S} T_\mathrm{S} + b, \tag{4}$$

where, T is the temperature for the mesh node, a and b is coefficients. Every node in the mesh layout owns the same heat conduction equation as Eq. (4). There are five unknown node temperatures in each equation. Simultaneously solving the temperature equations of all nodes is time-consuming. For saving computer memory and calculation time, the conduction equations shall be solved sector by sector. The node temperatures in one radial sector are solved together assuming that the node properties of the west and east sectors apply the values at the last iteration

$$a_\mathrm{P} T_\mathrm{P}^{(n)} = a_\mathrm{N} T_\mathrm{N}^{(n)} + a_\mathrm{S} T_\mathrm{S}^{(n)} + a_\mathrm{E} T_\mathrm{E}^{(n-1)} + a_\mathrm{W} T_\mathrm{W}^{(n-1)} + b. \tag{5}$$

Eq. (5) has only three unknown parameters and can be solved by Tridiagonal Matrix Algorithm (TDMA) with the corresponding boundary conditions [7]. When the solution of one radial sector is finished, physical properties of the nodes are updated. The radial heat conduction calculation is conducted in the next sector clock wise until all the node temperatures satisfy the convergence criterion (for each node, temperature difference $< 1\,^\circ\mathrm{C}$ between two iterations). In this way, the 2D heat conduction solution is transferred as many 1D solutions and the calculation efficiency can be greatly promoted.

B. Development of radiation heat transfer model

As a boundary condition for heat conduction solution, the radiation heat transfer inside the HEC is highly related to the fuel configuration. The cross section of an HEC channel is illustrated in Fig. 2. The radiation enclosure consists of outer surface of the central channel, surfaces of the fuel rods in the inner and outer rings, and the tube liner. The method of solving radiation heat transfer adopted by RELAP5 is referred [8]. The following assumptions are made:

1. Radiation heat transfer between different elevations is ignored.
2. All surfaces in the system are diffusive and grey;
3. Radiation exchange between water steam and fuel surface do not produce a big effect on the LOCA/LOECC result,

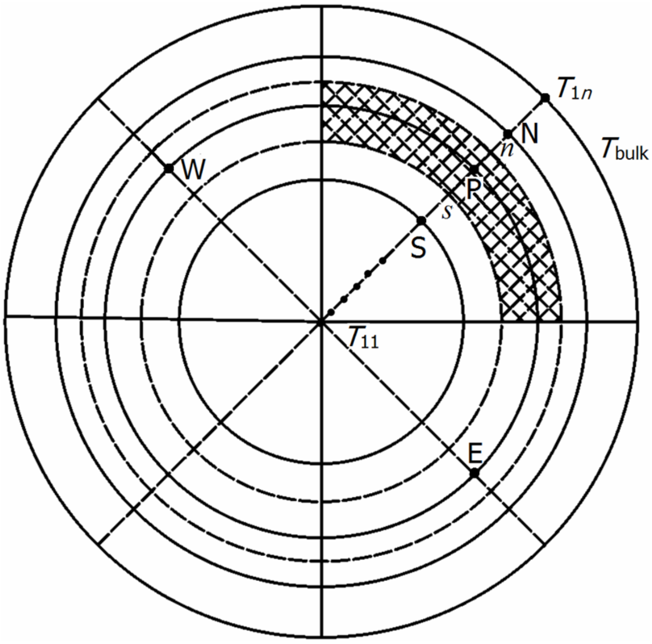

Fig. 1. Mesh layout of the heat structure.

and coolant in the pressure tube neither emits nor absorbs radiant thermal energy;

4. Reflectance from a surface is independent of the reflected direction and the radiation frequency.

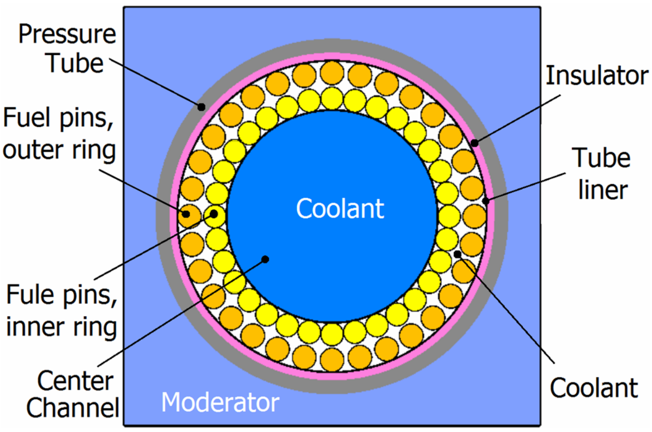

Fig. 2. (Color online) Cross-section of the high efficiency channel(HEC).

1. Net radiation heat flux

The radiosity of a surface is the radiant energy flux leaving a surface (i.e., the emitted energy flux plus the reflected energy flux). Energy balance for the i^{th} surface is

$$R_i = \varepsilon_i \sigma T_i^4 + \eta_i \sum_{j=1}^{n} R_j \frac{A_j}{A_i} F_{ji}, \tag{6}$$

where, R is radiation heat flux, σ is Boltzmann coefficient, η is reflectivity, A_i is area of surface i, A_j is area of surface j, and F_{ji} is the view factor from surface j to surface i. Considering the energy conservation law, we have

$$A_i F_{ij} = A_j F_{ji}, \tag{7}$$

where, F_{ij} is the view factor from surface i to surface j. Substituting Eq. (7) into Eq (6), we have

$$R_i = \varepsilon_i \sigma T_i^4 + \eta_i \sum_{j=1}^{n} R_j F_{ij} \tag{8}$$

The net heat flux at surface i, Q_i, is the difference between the radiosity of surface i and radiosity throwing to surface i from all surfaces, and it's given by

$$Q_i = R_i - \sum_{j=1}^{n} R_j F_{ij} \tag{9}$$

Combining Eqs. (8) and (9), the net heat flux of surface i is expressed by

$$Q_i = \frac{\varepsilon_i}{\eta_i}(\sigma T_i^4 - R_i) \tag{10}$$

In Eq. (10), the reflectivity and emissivity are the basic physical properties of surface i. By conservation of energy, the value sum of the reflectivity and emissivity for a sector equals to 1. In the calculation, the surface temperature at the previous time step is applied, and therefore, the radiosity is calculated explicitly.

2. Radiosity solution

On the basis of Eq. (8), the radiosity of all the surfaces can be calculated by:

$$\begin{cases} i=1: (1-\eta_1 F_{11})R_1 + (0-\eta_1 F_{12})R_2 + (0-\eta_1 F_{13})R_3 \cdots + (0-\eta_1 F_{1n})R_n = \sigma \cdot \varepsilon_1 T_1^4 \\ i=2: (0-\eta_2 F_{21})R_1 + (0-\eta_2 F_{22})R_2 + (0-\eta_2 F_{23})R_3 \cdots + (0-\eta_2 F_{2n})R_n = \sigma \cdot \varepsilon_2 T_2^4 \\ \vdots \\ i=i: (1-\eta_i F_{i1})R_1 + (0-\eta_i F_{i2})R_2 \cdots (0-\eta_i F_{ii})R_i \cdots\cdots (0-\eta_i F_{in})R_n = \sigma \cdot \varepsilon_i T_i^4 \\ \vdots \\ i=n: (0-\eta_n F_{n1})R_1 + (0-\eta_n F_{n2})R_2 + (0-\eta_n F_{n3})R_3 \cdots + (0-\eta_n F_{nn})R_n = \sigma \cdot \varepsilon_n T_n^4 \end{cases} \tag{11}$$

The surface emissivity is regarded as constant. From [4], surface emissivity of the central channel is 0.34 and the emissivity of the fuel rod and the liner is 0.8. For a grey body, absorptivity equals emissivity and hence "$\eta = 1 - \varepsilon$", which would simplify the formula. Due to the central symmetry of the fuel assembly (Fig. 2), the pressure tube and the center channel are circumferentially divided into 32 sectors and each fuel rod is divided into 4 sectors. With the view factor of each surface calculated by GEOFAC code [9], the radiosity matrix can be solved, and the net radiation heat flux can be obtained using Eq. (11).

C. Heat conduction solution considering the effect of radiation and convection

The net heat flux created by radiation and convective heat transfer is used as the boundary condition of the 2-D heat conduction,

$$-\lambda \frac{\partial T}{\partial r}\bigg|_i = h_i(T_i - T_{sk}) + Q_i \tag{12}$$

The radiation heat flux Q_i in Eq. (12) is also a function of surface temperature. The bulk-fluid temperature for all the sectors in an enclosure is assumed to be the same. The natural convection heat transfer coefficient inside the HEC is calculated by Churchill-Chu correlation [10]. The forced convection heat transfer in the HEC is mainly calculated by Dittus-Boelter correlation [11] at subcritical pressure and Jackson correlation [12] at supercritical pressure in the process of LOCA/LOECC. To simplify the solution, surface temperatures at the previous time step are adopted to compute the radiation heat flux explicitly and therefore the iteration solution of the radiation heat flux is avoided.

III. VERIFICATION OF SCTRAN RADIATION HEAT TRANSFER MODEL

Due to the lack of experimental data, verification of the radiation heat transfer model was done by code to code comparison with Canadian system code CATHENA. As a one-dimensional and two-fluid thermal-hydraulic code [9], it includes 1D and 2D heat conduction models (GENHTP). Its ability to evaluate the radiation heat transfer has been validated by Lei and Goodman [13].

The 64-element Canadian-SCWR bundle was analyzed for the verification. The HEC cross-section is shown in Fig. 2. The buddle power was 9.34 MW. The fuel pins of the inner and outer rings occupied 44% and 56% of the power, respectively. Temperature of the moderator outside the pressure tube was 80 °C and heat transfer coefficient between moderator and pressure tube was 1000 W/(m^2 K). Three steady-state cases with different decay heat levels (2%, 3% and 4% of the rated power) were simulated by SCTRAN and CATHENA, respectively. In the simulations, the decay heat was transferred from the fuel rod to inner surface of the pressure tube only by radiation heat transfer. Each sector in the HEC was marked by a number (Fig. 3).

Table 1 lists the surface temperatures of the 64-element fuel bundle at 2%, 3% and 4% power levels calculated by SCTRAN and CATHENA. The SCTRAN results agree well with those of CATHENA, differing with the maximum absolute error of 6.1 °C and the biggest relative error of 0.9%. This shows that the 2D heat conduction and radiation heat transfer models developed for SCTRAN are of guaranteed calculation accuracy.

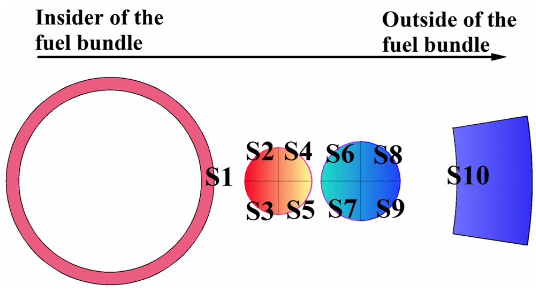

Fig. 3. (Color online) Numbering of the HEC surfaces.

IV. SAFETY ANALYSIS OF LOCA/LOECC

The ability to maintain core components below the melting temperatures in postulated accident is referred to as the concept of "no-core-melt", which is an important safety goal for Canadian-SCWR. The accident of LOCA with a loss of ECCS was simulated with the modified SCTRAN to evaluate whether Canadian-SCWR has the potential to achieve the goal of "no-core-melt".

A. Introduction to Canadian-SCWR

The conceptual Canadian-SCWR design possesses a modular design that separates the coolant from the moderator, as in the CANDU reactors. The reactor core consists of 336 fuel channels, each housing a 5-m long fuel assembly. It is designed to generate 2540 MW of thermal power or about 1200 MW of electric power. In the conceptual design (Fig. 4), light water coolant enters the inlet plenum. It flows downward the central flow tube of the channel. Near the channel bottom, the coolant exits the central flow tube, flows upward to pass through the fuel elements (fuel assembly), and arrives at the outlet plenum. From the outlet plenum, the high-temperature and high-pressure coolant is fed to the high pressure turbine. The cylindrical vessel houses the relatively low-pressure and low-temperature heavy water moderator. The main parameters of the Canadian-SCWR are listed in Table 2.

HEC is adopted for Canadian-SCWR conceptual design. It consists of a pressure tube, an outer liner tube, an insulator and an inner liner tube. The pressure tube is surrounded by heavy water moderator. A potential advantage of using the HEC is that in the unlikely event of a LOCA/LOECC, the

TABLE 1. Surface temperatures (in °C) of the HEC channel calculated by SCTRAN and CATHENA at different power levels

	Power levels	S1	S2	S3	S4	S5	S6	S7	S8	S9	S10
SCTRAN	2%	1258.3	1263.8	1263.8	1236.2	1236.2	1195.8	1195.8	1125.6	1125.6	324.9
	3%	1442.8	1449.1	1449.1	1411.9	1411.9	1371.4	1371.4	1277.3	1277.3	450.1
	4%	1591.1	1598.2	1598.2	1552.3	1552.3	1512.4	1512.4	1398.9	1398.9	577.5
CATHENA	2%	1253	1258	1258	1233	1233	1191	1191	1127	1127	328
	3%	1437	1443	1443	1408	1408	1367	1367	1279	1279	454
	4%	1585	1592	1592	1549	1549	1508	1508	1401	1401	582

TABLE 2. Main parameters of Canadian-SCWR

Core pressure (MPa)	25
Thermal/Electrical power(MW)	2540/1200
Efficiency (%)	45-50
Inlet/outlet temperatures (°C)	350/625
Fuel channel number	336
Fuel bundle type	64-element
Neutron spectrum/reactor type	Thermal/pressure-tube
Coolant	light water
Moderator	heavy water
Main coolant flowrate(kg/s)	1254
Active core height(m)	5.0
Cladding material	Stain steel(SS310)

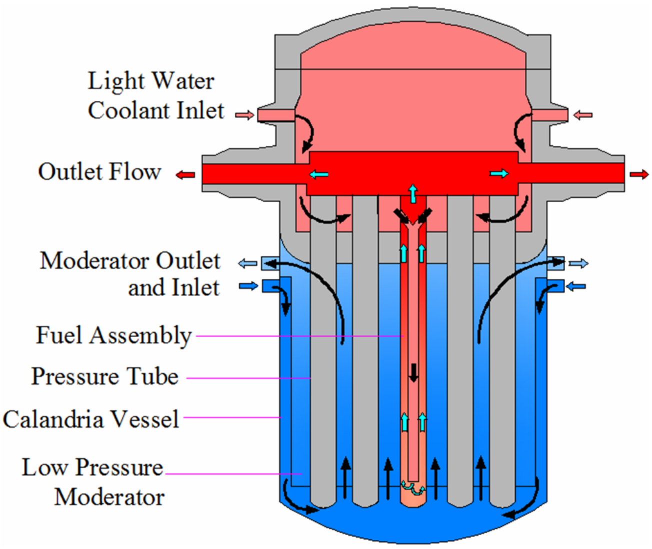

Fig. 4. (Color online) Schematic of Conceptual Canadian SCWR Core.

heat in the fuel would be transferred by thermal radiation to the liner tube and then conducted to the moderator through the insulator. The 64-element fuel bundle with two concentric rings is equipped inside the pressure tube.

B. SCTRAN model

The SCTRAN model idealization of Canadian-SCWR was developed based on the conceptual design. In order to simulate more accurately the effect of the radial power distribution, the 336 channels in the reactor core are divided into four groups (84 channels each), namely the "average power channels (AP)", "high power channels (HP)", "medium power channels (MP)" and "low power channels (LP)" [14], as shown in Fig. 5 in the radial direction, In the axial direction, the fuel bundles and the coolant channel are divided into 10 parts. The axial power distribution for fuel bundle refers [14]. Fuel pins of the inner and outer rings of each group are simulated by independent heat structures, which exchange heat separately with the coolant.

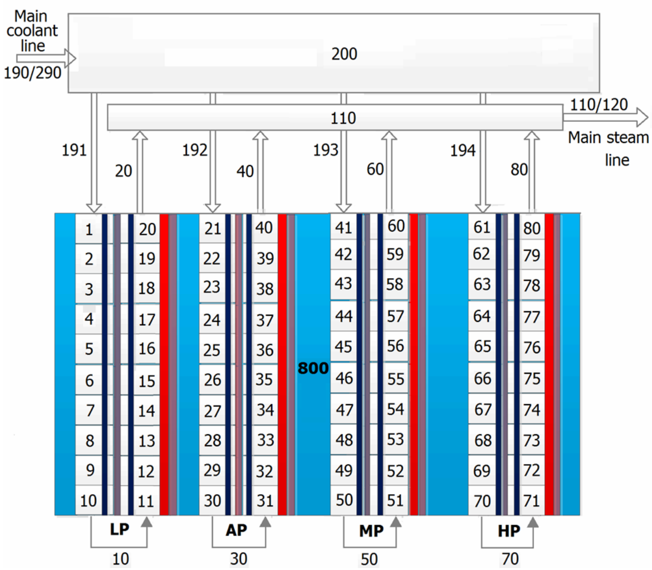

Fig. 5. (Color online) SCTRAN idealization of Canadian-SCWR concept. The control volumes are numbered as 1–80.

The heat exchange between central channel and coolant channel is also taken into consideration. A time dependent junction at 350 °C and 1254 kg/s, and a time dependent volume at 625 °C and 25 MPa, are set as the boundary conditions of the main coolant line and main steam line, respectively. The moderator cooling system contains an active and a passive moderator cooling system. In the accident conditions, only passive moderator cooling system (PMCS) is used [15]. The PMCS is simulated by volume 800 (Fig. 5), serving as an ultimate heat sink. It will be active automatically during transients. Thus, moderator temperature of 80 °C is assumed and a constant heat transfer coefficient of 1000 W/(m^2 K) between the moderator and the pressure tube is applied [3], which indicates that the moderator removes the core heat through natural convection. There is no active system preparing for the Canadian-SCWR system when LOCA/LOECC occurs. The moderator system is assumed to keep intact in the whole process. Turbine stop valves are installed on the main steam lines, which are tripped by the "power scram" signal. Other initial conditions and assumptions are as follows:

– The reactivity feedback in the core is neglected in both steady and accident simulations.

– The decay heat is calculated by referring to the previous paper [16].

– The emissivity of the fuel sheath and liner tube is 0.8 while the emissivity of central channel is 0.34.

– The natural convection heat transfer coefficient in the HEC is calculated by Churchill-Chu correlation [10];

– Referring to the ASM specialty handbook [17], melting temperature of SS310 is 1400–1450 °C. Thus, the melting temperature of the fuel cladding is set as 1400 °C.

– Due to the radiation heat transfer effect, each fuel sheath had four sector temperatures. The maximum sector temperature is applied to describe the surface temperature variation.

C. Results for LOCA/LOECC

The core will lose most of its inventory and suffers a cooling deteriorate condition when LOCA occurs. The heat in the fuel could only be removed by the passive natural convection of the high temperature steam and the thermal radiation exchange between the fuel sheath and the liner tube, while ECCS is lost simultaneously. In this process, the radiation heat transfer plays a dominant role. The double-ended break accident at the cold leg is analyzed because it is the most severe LOCA accident. As the HP group is of the largest power fraction and the highest cladding temperature, it is selected to be the main analysis object in the current analyses.

In the simulation, the break at the cold-leg occurred at 0.5 s. At 1 s, the control rods started to drop and the core power decreased. At the same time, the turbine stop valve was closed. The coolant flowrate from the main coolant pump was maintained in the first 10 s and then decreased to zero within 5 s (actually decided by the pump inertia).

Fig. 6(a) shows the coolant flowrate through the break. When the break occurred, large amount of coolant were drained out through the break at a critical velocity. The core pressure decreased quickly to the subcritical level because of the loss of coolant. The coolant flowrate in the different channels are shown in Fig. 6(b). The break located in the cold leg resulted in the reversed flow in each channel. Large amount of coolant of 625 °C from the outlet plenum was directed to the fuel channel, which led to a greatly degraded cooling condition. Therefore the fuel sheath temperatures increased quickly during this period.

Fig. 7(a) shows the heat removed from the fuel rings and the heat variation in the HP group in the first 50 s. Fig. 7(b) shows the maximum cladding surface temperature (MCST) of the components. At first, the nuclear power produced in the fuel rods cannot be totally removed to coolant and the MCST of both rings increased sharply. With the power decreasing

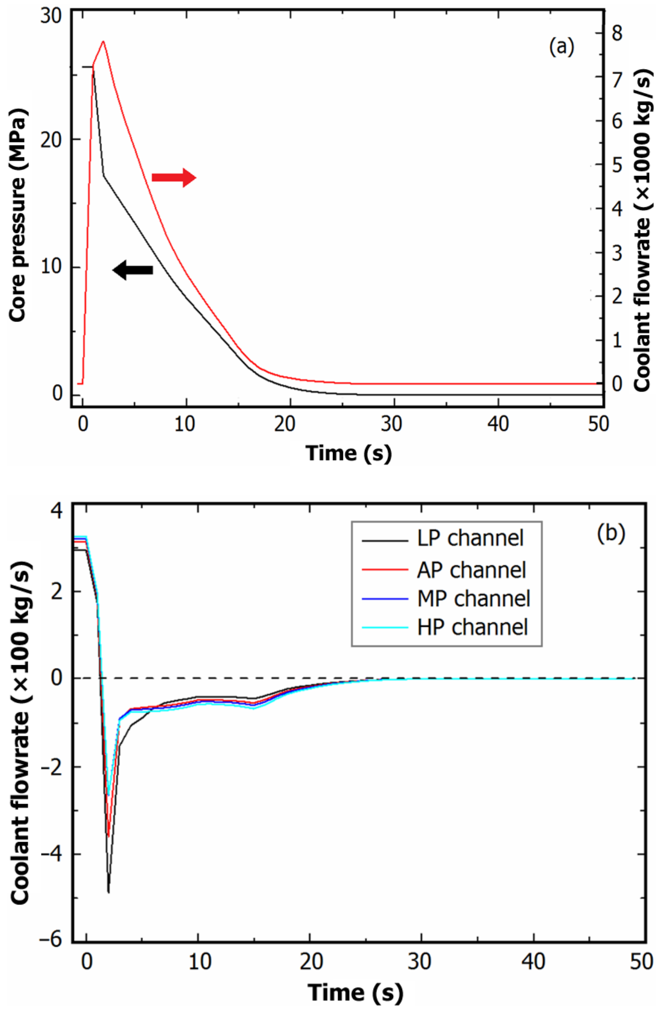

Fig. 6. (Color online) The core pressure and break coolant flowrate (a), and coolant flowrate of the four flow channels (b), in the first 50 s of LOCA.

and the reversed flow being established, MCSTs kept a slower increasing trend, but dropped a little at about 15 s. However, when the coolant in outlet plenum was exhausted, the cooling conditions in the coolant channel deteriorated. The channels were filled with high-temperature steam and the radiation heat transfer became dominant in the HEC at around 30 s. The heat transferred by radiation and natural convection at this time was not large enough to remove the decay heat of the inner rings, while the decay heat of the outer rings can be totally removed. MCST of the inner ring started to rise again at around 15 s while that of the outer ring kept decreasing. Due to protection from insulator, the pressure tube surface remained at about 200 °C.

With time went on, the fuel cladding temperature of the inner ring increased continuously while the outer ring experienced an MCST decrease. As shown in the Fig. 8, MCST of the inner ring of the HP group started to drop slowly after reaching the peak value of 1236 °C. The fuel rod would reach a steady state when the heat removed by radiation and convection equals to the decay heat. However, the decay heat

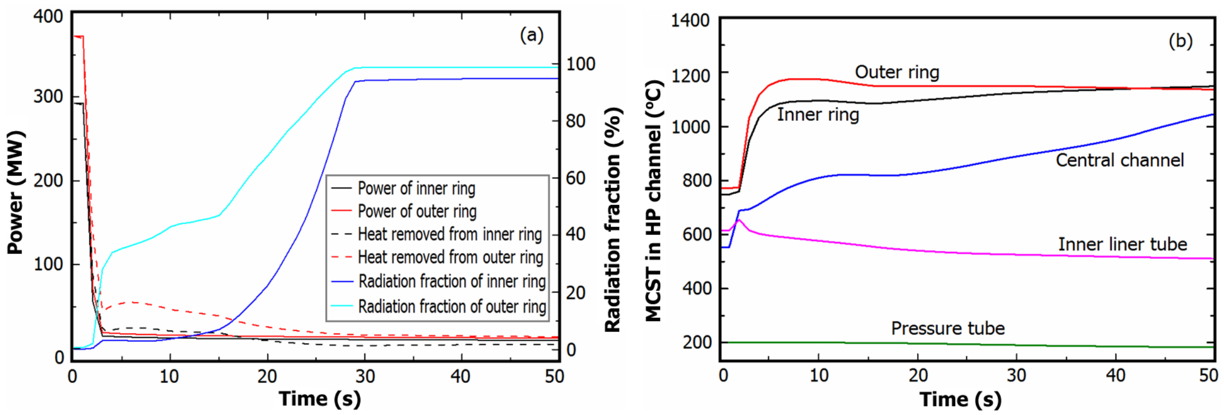

Fig. 7. (Color online) Power decay and heat removed from the fuel rings (a) and MCST in the HP group (b), in the first 50 s of LOCA.

decreased slowly with time, which resulted in the continuous decrease of the MCST. Likewise, the behaviors of the other three power groups are similar to that of the HP group, which is of the highest MCST because of its highest power fraction.

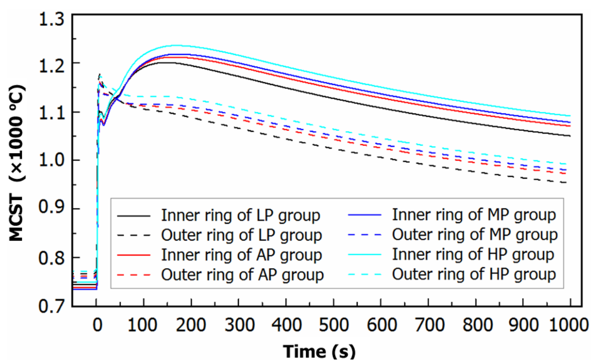

Fig. 8. (Color online) MCST vs time in all the coolant channels.

According to the above analysis, the decay heat of the Canadian-SCWR fuel pins in the process of LOCA/LOECC can be transferred to the moderator outside the pressure tube thourgh natural convection and radiation heat transfer. The fuel rods of the two rings experience different sheath temperature variation. The fuel rods in the outer ring is closer to the pressure tube and its radiation heat exchange with the pressure tube is enhanced. While the radiation heat transfer for the fuel rods in the inner ring is worse than that of the outer ring. That is the reason why fuel rods in the inner ring experience a longer period of sheath temperature increase. The peak cladding temperature of the two rings are 1236.3 °C and 1177.3 °C respectively, which are much lower than the melting temperature of the fuel cladding.

V. CONCLUSION

This paper focuses on the assessment of the inherent safety of 64-element Canadian-SCWR. A two-dimensional heat conduction model and a radiation heat transfer model are developed and incorporated successfully into SCTRAN. Meanwhile, the validity of the newly developed models for SCTRAN is verified by CATAENA, which is a system code developed by AECL.

A SCTRAN idealization of the Canadian-SCWR conceptual design has been developed. Using the SCTRAN idealization developed for Canadian-SCWR, a simulation of the steady-state thermal-hydraulic conditions is performed. In LOCA/LOECC, with total loss of core coolant inventory, radiation heat exchange among sheaths and the natural convection of the high-temperature steam can removed certain amount of core decay heat. On the basis of conservative assumption, the maximum fuel sheath temperatures in the inner and outer rings of the HP group are 1236 °C and 1177 °C, respectively, which are lower than the melting point of the cladding material. The results show that the Canadian SCWR is capable of achieving the design object of “no-core-melt” under LOCA/LOECC.

ACKNOWLEDGMENTS

The authors appreciate the support of Laurence K H Leung from AECL, Feng Jia and Zhang Guomin from Xi’an Jiaotong University.

[1] Leung L K H. Termalhydraulics and safety programs in support of the CANDU SCWR design, Proceedings of the international conference on nuclear engineering, ICONE18, Xi’an, China, 2010.
[2] Vasic A and Khartabil H F. Passive cooling of the CANDU SCWR fuel at LOCA / LOECC conditions, Proceedings of

GLOBAL, Atomic Energy Society of Japan, Tsukuba, Japan, 2005.

[3] Shan J, Jiang Y and Leung L K H. Subchannel and radiation heat transfer analysis of 54-element CANDU-SCWR bundle, the 5^{th} international symposium on supercritical water cooled reactors (ISSCWR-5), Vancouver, British Columbia, Canada, March 13-16, 2011.

[4] Licht J and Xu R. Preliminary no-core melt assessment for the high efficiency channel preconceptual design, The 3^{rd} China-Canada joint workshop on supercritical-water-cooled reactors, CCSC-2012, Xi'an, China, 2012.

[5] Wu P, Gou J, Shan J, *et al*. Safety analysis code SCTRAN development for SCWR and its application to CGNPC SCWR. Ann Nucl Energy 2013, **56**: 122–135. DOI: 10.1016/j.anucene.2013.01.028

[6] Wu P, Gou J, Shan J, Zhang B, *et al*. Preliminary safety evaluation for CSR1000 with passive safety system. Ann Nucl Energy, 2014, **65**: 390-401. DOI: 10.1016/j.anucene.2013.11.031

[7] Yang S and Tao W. Heat transfer. Beijing(China): Higher Education Press, 2006.

[8] The RELAP5 code development team. RELAP5/MOD3 code manual. 1995.

[9] The CATHENA dode development team. CATHENA MOD-3.5d theory manual. 2005.

[10] Churchill S W and Chu H H S. Correlating equations for laminar and turbulent free convection from a vertical plate. Inter J Heat Mass Tran, 1975, **18**: 1323–1329. DOI: 10.1016/0017-9310(75)90243-4

[11] Dittus F W and Boelter L M K. Heat transfer in automobile radiators of the tubular type. University of Ca1ifornia Pub1ications in Engineering, 1930, **2**: 443–461. DOI: 10.1016/0735-1933(85)90003-X

[12] Hall W B and Jackson J D. Heat transfer near the critical point. Adv Heat Transfer, 1971, **7**: 1–86.

[13] Lei Q M and Goodman T M. Validation of radiation heat transfer in CATHENA. International Conference on Simulation Methods in Nuclear Engineering, Montreal, Canada, Sep. 8-11 1996.

[14] Wang D F and Wang S. A Cathena model of the Canadian SCWR concept for safety analysis. the 6^{th} international symposium on supercritical water cooled reactors (ISSCWR-6), Shenzhen, Guangdong, China, March 3-7, 2013.

[15] Novog D and McGee G. Safety concepts and systems of the Canadian SCWR. the 3rd China-Canada joint workshop on supercritical-water-cooled reactors (CCSC-2012), Xi'an, China, April 18-20, 2012.

[16] Pencer J, McDonald M and Anghel V. Parameters for transient response modeling for the Canadian SCWR. The 19^{th} Pacific basin nuclear conference (PBNC 2014), Hyatt Regency Hotel, Vancouver, British Columbia, Canada, Aug. 24-28, 2014.

[17] Davis J R. ASM specialty handbook: Stainless steels. Ohio(USA): ASM International, Materials Park, 1994. DOI: 10.1002/maco.19950460815